Detection of vibrationally excited methyl formate in W51 e2

Karine Demyk, Georges Wlodarczak, Miguel Carvajal

Astronomy & Astrophysics manuscript no. mtf-exi-revised-2.hyper30618
July 17, 2008

Detection of vibrationally excited methyl formate in W51 e2

K. Demyk[1⋆], G. Wlodarczak[1], and M. Carvajal[2]

[1] Laboratoire de Physique des Lasers, Atomes et Molécules, UMR CNRS 8523 Université Lille 1, F-59655 Villeneuve d'Ascq Cedex
e-mail: Karine.demyk@cesr.fr
[2] Departamento de Fisica Aplicada, Facultad de Ciencias Experimentales, Universidad de Huelva, 21071 Huelva, Spain

Received 7 January 2008; accepted 30 June 2008

ABSTRACT

Context. Hot cores in molecular clouds, such as Orion KL, Sgr B2, W51 e1/e2, are characterized by the presence of molecules at temperature high enough to significantly populate their low-frequency vibrationally excited states. For complex organic molecules, characterized by a dense spectrum both in the ground state and in the excited states, such as methyl formate, ethyl cyanide or dimethyl ether, lines from vibrationally excited states certainly participate to the spectral confusion.
Aims. Thanks to the recent laboratory study of the first torsional excited mode of methyl formate, we have searched for methyl formate, $HCOOCH_3$, in its first torsionally excited state (υ_t=1) in the molecular cloud W51 e2.
Methods. We have performed observations of the molecular cloud W51 e2 in different spectral regions at 1.3, 2 and 3 mm with the IRAM 30 m single dish antenna.
Results. Methyl formate in its first torsionally excited state (υ_t=1 at 131 cm^{-1}) is detected for the first time toward W51 e2. 82 transitions have been detected among which 46 are unblended with other species. For a total of 16 A-E pairs in the observed spectrum, 9 are unblended; these 9 pairs are all detected. All transitions from excited methyl formate within the observed spectral range are actually detected and no strong lines are missing. The column density of the excited state is comparable to that of the ground state. For a source size of 7″we find that T_{rot} = 104 ± 14 K and N = $9.4^{+4.0}_{-2.8} \times 10^{16}$ cm^{-2} for the excited state and T_{rot} = 176 ± 24 K and N = $1.7^{+.2}_{-.2} \times 10^{17}$ cm^{-2} for the ground state. Lines from ethyl cyanide in its two first excited states (υ_t=1, torsion mode at 212 cm^{-1}) and (υ_b=1, CCN in-plane bending mode at 206 cm^{-1}) are also present in the observed spectrum. However blending problems prevent a precise estimate of its abundance. However as for methyl formate it should be comparable with the ground state for which we find T_{rot} = 103 ± 9 K and N = $3.7^{+0.6}_{-0.4} \times 10^{15}$ cm^{-2} for a 7″source size.
Conclusions. With regard to the number of lines of excited methyl formate and ethyl cyanide detected in W51 e2, it appears that excited states of large molecules certainly account for a large number of unidentified lines in spectral survey of molecular clouds.

Key words. Line: identification – Methods: observational – ISM: molecules – ISM: abundances – ISM: individual objects: W51 e2 – Radio lines: ISM

1. Introduction

W51 e2 is a hot core part of the W51 H_{II} region located in the Sagittarius spiral arm at a distance of about 7-8 kpc. It is a region of high-mass star formation. W51 e2 and W51 e1 are thought to be important star-forming cores. They exhibit a rich chemistry, comparable to that observed in Orion or in Sagittarius. Numerous large organic molecules have been observed towards them. CH_3CN and CS maps were studied by Zhang et al. (1998). Formic acid (HCOOH) was mapped by Liu et al. (2001). Methyl formate ($HCOOCH_3$) and ethyl cyanide (CH_3CH_2CN) were observed in several studies (Liu et al. 2001; Ikeda et al. 2001; Remijan et al. 2002). Ikeda et al. (2001) studied ethylene oxide (c-C_2H_4O) and its isomer acetaldehyde (CH_3CHO). Acetic acid (CH_3COOH) was detected by Remijan et al. (2002) with a fractional abundance of (1-6) × 10^{-2} relative to $HCOOCH_3$. Glycine, whose presence may be suggested from the observations of acetic acid with which it shares common structural elements, was not detected in W51 e2 (Snyder et al. 2005). Recently, trans-ethyl methyl ether was detected in W51 e2 (Fuchs et al. 2005).

The rotational temperature of most of these large molecular species is high. Liu et al. (2001) estimated the rotational temperature in W51 e2 to be in the 200-300 K range. From high resolution observations of CH_3CN analyzed with statistical equilibrium models, Remijan et al. (2004) derived the kinetic temperature in W51 e2 to be T_{kin} = 153(21) K. At such temperature, low-energy vibrational excited states can be significantly populated. Transitions from vibrationally excited states have indeed been observed in other sources such as in Sgr B2(N-LMH) for C_2H_3CN, CH_3CH_2OH (Nummelin et al. 1998) and CH_3CH_2CN (Mehringer et al. 2004). Recently, lines from torsionally excited methyl formate have been identified in Orion KL (Kobayashi et al. 2007).

In this study we present the first detection of excited methyl formate and ethyl cyanide in the molecular cloud W51 e2. The initial project was to look for methyl carbamate (NH_2COOCH_3), an isomer of glycine (NH_2CH_2COOH) which has a larger dipole moment, making its detection more favorable than glycine. It was not detected. However, few strong unidentified lines in the data attracted our attention and were possibly attributed to methyl formate in its first torsional excited state. Further observations confirmed this detection and also lead to the detection of excited ethyl cyanide in W51 e2. The first vibrationally excited state of methyl formate is the CH_3 torsion mode, ν_{18}, hereafter called υ_t=1, at 131 cm^{-1} (188 K). The rotational spectrum in

Send offprint requests to: K. Demyk, e-mail: karine.demyk@cesr.fr
⋆ *Present address: Centre d'Etude Spatiale des Rayonnements, Université Paul Sabatier, F-31028 Toulouse, France*

this excited state was measured and analyzed by Ogata et al. (2004). Ethyl cyanide has two close vibrationally excited states, the CCN in-plane bending mode, ν_{13}, hereafter called υ_b=1, at 206 cm^{-1} (296 K) and the CH_3 torsion mode, ν_{21}, hereafter called υ_t=1, at 212 cm^{-1} (305 K). A preliminary analysis of the rotational spectrum in these two excited states is presented in the paper from Mehringer et al. (2004).

The observations and the methods used for the data analysis are described in Sect. 2 and Sect. 3, respectively. The study of methyl formate and ethyl cyanide in the ground and excited state is presented in Sect. 4 and Sect. 5, respectively. The search for methyl carbamate and glycine is presented in Sect. 6. The discussion is carried out in Sect. 7.

2. Observations

The observations were performed with the IRAM 30m antenna at Pico Veleta (Spain) in June 2003 and June 2006. W51 e2 was observed at the position $\alpha(2000) = 19°23'43.9''$and $\delta(2000) = 14°30'34.8''$in position switching mode with the OFF position located at $\alpha = 300\,''$and $\delta = 0\,''$.

Several spectral windows in the 80-250 GHz range were observed in order to include as many transitions as possible for the searched molecules (excited methyl formate and ethyl cyanide for the 2006 data and methyl carbamate and glycine for the 2003 data) and as few transitions as possible of other molecules having numerous strong lines (such as methyl formate and ethyl cyanide in the ground state, dimethyl ether, etc.).

All lines were observed with an array of 4 receivers (in single side band mode) set at the appropriate frequencies. The spectrometers used are a low resolution 1 MHz filter bank and an autocorrelator with a spectral resolution in the 40-320 kHz range, split between different receivers. Focus and pointing were regularly checked on the nearby ultra compact HII region K 3-50A. The rejection of the image band (USB) was of about 26 dB at 3 mm, 12 dB at 2 mm, 15 dB at 1.3 mm and 10 dB at 1.1 mm. The system temperature was typically 100-200 K, 200-700 K, 200-700 K and 400-1500 K at 3, 2, 1.3 and 1.1 mm, respectively. The total usable ON+OFF integration time varies from 30 to 50 minutes depending on the frequency range. The beam size is 22 $''$, 17 $''$and 10.5 $''$at 3, 2 and 1.3 mm, respectively. The spectra are presented in main beam temperature unit which is calculated from the antenna temperature: $T_{mb} = F_{eff}/B_{eff} \times T_A{}^*$. The data were reduced using the GILDAS package.

3. Analysis

For the data analysis we assume that local thermodynamic equilibrium (LTE) is reached, i.e. we assume that the excitation, rotational and vibrational temperatures are equal to the kinetic temperature in the emitting region and that the lines are thermalized, i.e. their level population is described by a Boltzmann distribution at that temperature. The validity of this assumption will be discussed later in Sect. 7.

The data were analyzed using the classical rotational diagram method to estimate the rotational temperature and the column density together with their uncertainties for the different identified species. We adopt the formulation from Turner (1991), corrected for beam dilution effects:

$$\ln\left(\frac{3kW}{8\pi^3\nu S\mu^2 g_i g_k}\right) = \ln\left(\frac{N}{Q}\right) - \frac{E_u}{kT} - \ln(b) \quad (1)$$

where W is the integrated line intensity in K.km.s^{-1}, ν the line frequency, $S\mu^2$ the line strength in Debye^2, g_i the reduced nuclear spin statistical weight, g_k the K-level degeneracy, Q is the partition function, E_u the upper state energy, N is the total column density and T the excitation temperature. Assuming a gaussian beam, the beam dilution factor b is given by:

$$b = \frac{\theta_s^2}{\theta_s^2 + \theta_{tel}^2} \quad (2)$$

where θ_s and θ_{tel} are, respectively, the source and telescope beam size in arcsecond.
Beam dilution effects were taken into account both in the rotational diagram analysis and in the emission modeling (see below). The emission region in W51 e2 is observed to be smaller than 10$''$for most organic molecules (Remijan et al. 2002; Liu et al. 2001). Consequently beam dilution effects are important at low frequency at which the IRAM 30m antenna beam size is significantly larger (29$''$at 86 GHz).

We have compared the observed spectrum with simulated spectra calculated using a simple emission model at local thermodynamic equilibrium (LTE). The expression for the simulated main beam temperature for one molecule is thus:

$$T_{mb} = b \times (J - J_{bg}) \times (1 - e^{-\tau}) \quad (3)$$

where J is the source function:

$$J = \frac{h\nu}{k} \times (e^{h\nu/kT} - 1)^{-1} \quad (4)$$

and

$$J_{bg} = \frac{h\nu}{k} \times (e^{h\nu/k\times 2.7} - 1)^{-1} \quad (5)$$

τ is the optical depth, summed over all the transitions of the molecules:

$$\tau = \sum_i \frac{c^2}{8\pi\nu^2} N_{tot} \frac{g_u}{Q} A_{ul} \Phi(\nu) e^{-E_l/kT} (1 - e^{-E_{ul}/kT}) \quad (6)$$

and $\Phi(\nu)$ is the line profile:

$$\Phi(\nu) = \frac{1}{\sqrt{\pi}\Delta\nu_D} \times e^{-(\nu-\nu_i)^2/\Delta\nu_D^2} \quad (7)$$

A_{ul} is the Einstein coefficient, E_{ul} the energy of the transition, E_l the energy of the lower state, g_u is the upper state degeneracy, Q the partition function, $\Delta\nu_D$ is the Doppler width of the line, b is the beam dilution correction factor and N_{tot} is the total column density.

In hot cores, the temperature is such that the low-energy vibrational and/or torsional excited modes are significantly populated. Consequently we have used the vibrational-rotational partition function, Q_{rv}, instead of the pure rotational partition function. Assuming non-interacting harmonic vibrational levels and rigid rotor levels, the ro-vibrational partition function is approximated by (see Gordy & Cook 1984):

$$Q_{rv} = \prod_i (1 - e^{-h\nu_i/kT})^{-d_i} \times Q_{rot} \quad (8)$$

where ν_i is the frequency of the vibrational mode i, d_i its degeneracy, and Q_{rot} is the rotational partition function. Q_{rot} is approximated by:

$$Q_{rot} = \sigma \times \sqrt{\frac{\pi (kT)^3}{h^3 ABC}} \quad (9)$$

where σ is the symmetry number (see Gordy & Cook 1984). At LTE, the temperature used to calculate the rotational and vibrational partition function is the same, we thus implicitly assume that $T_{vib} = T_{rot}$, an hypothesis which may not be valid (see Sect.7). For methyl formate which has one internal rotor, rotational transitions are split into A and E components and σ is equal to 2. To calculate the partition function, we have considered the first excited state of methyl formate at 131 cm^{-1}. For ethyl cyanide, we have used the partition function given by Mehringer et al. (2004) which is calculated by summing the rotational states of the ground state and of the first two excited states of ethyl cyanide at 206 and 212 cm^{-1}. For methyl carbamate we have used the partition function in the ground vibrational state given by Groner et al. (2007).

4. Torsionally excited methyl formate

The prediction of the methyl formate lines is based on the most recent work on this species from Carvajal et al. (2007). In this work, all experimental data available on the ground and excited states (3496 and 774 microwave lines, respectively) in the 7-200 GHz frequency range, covering the J values up to 43 in the ground state and up to 18 in the first excited state υ_t=1, were collected from previously published studies (Ogata et al. 2004; Oesterling et al. 1999; Plummer et al. 1986, 1984; Demaison et al. 1984). Carvajal et al. (2007) also added 434 new lines of methyl formate in the ground state, measured in Lille in the 567-669 GHz spectral range and corresponding to transitions with J and K values up to 62 and 22, respectively. This dataset was fitted within almost experimental accuracy (root-mean-square deviations of 94 kHz and 84 kHz for the 3496 (774) lines of the ground torsional state and of the excited state υ_t=1, respectively) using the so-called rho axis method (RAM) described in the literature (Hougen et al. 1994) and a model extended to include perturbation terms through eighth order. The spectroscopic parameters and the details on the fitting procedure are given in the paper from Carvajal et al. (2007) in which a table presenting all the fitted experimental frequencies, measurement uncertainties, calculated frequencies, observed-calculated values , line strengths, energy levels as well as identification of the transitions, is available as Supplementary data.

For the detection in the W51 e2 spectrum, we have provided a line-list of predicted line-center frequencies and line intensities based on an internal rotation model (RAM or Rho Axis Method). This method and the code[1] developed was used for several molecules detected in the interstellar medium (acetaldehyde, CH_3COH, (Kleiner et al. 1996), acetamide CH_3CONH_2, (Hollis et al. 2006) and acetic acid CH_3COOH, (Ilyushin et al. 2007). The laboratory measurements and predicted line frequencies of transitions in the first excited torsional state υ_t=1 of methyl formate in the spectral range used in the present detection are presented in Table 1 together with the line

[1] A version of the program is available at the web site (http://www.ifpan.edu.pl/~kisiel/introt/introt.htm#belgi) and other versions can be available by I. Kleiner (see the web site for more information).

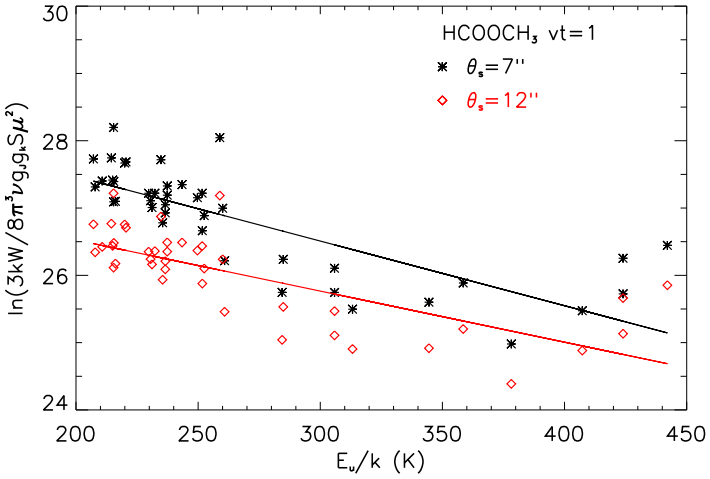

Fig. 2. Rotational diagram of the torsionally excited state of methyl formate for different source sizes. For a source size of 7″(black stars) we find a rotational temperature of T_{rot} = 104 ± 14 K and a column density of N = $9.4^{+4.0}_{-2.8} \times 10^{16}$ cm^{-2}; for a source size of 12″(red diamonds) we find T_{rot} = 131 ± 20 K and N = $3.4^{+1.5}_{-1.1} \times 10^{16}$ cm^{-2}.

assignment, the observed-calculated value, the experimental accuracy, the calculated uncertainty, the line strength and the energy of the lower level. [2]

More than eighty transitions from torsionally excited methyl formate, 82 precisely, are detected in the source among which 46 are not blended. Taking into account possible blending, we find that all lines from torsionally excited methyl formate predicted to be intense enough to be detectable are present in the observed spectra. Furthermore, no lines, such as unobserved strong lines, contradicts the identification in the observed spectral range. The internal rotation of the methyl group of methyl formate splits the transitions into A and E components having the same intensity. Among the 16 observed A-E pairs, 9 are not blended (see Fig. 1). The intensity of the lines in a A-E pair, when none of the lines in the pair is blended, is consistent with the expected ones, strengthening the identification of excited methyl formate in this source. The detected lines (observed frequency, integrated intensity and line intensity) are listed in Table 2 together with the laboratory or calculated frequency, the quantum numbers of the transition, its line strength and lower state energy. The first column of Table 2 indicates the line number which is used to label the lines in Fig. 1. The number in parenthesis points out the A or E line associated to the transition when it is observed. However about half of the lines are blended. Comments have been added in Table 2 to indicate line blenders when they are identified.

The non-blended lines have been used to estimate the rotational temperature and column density of excited $HCOOCH_3$ using the rotational diagram method (Fig.2, Table 4). Remijan et al. (2002) have mapped W51 e2 with BIMA in two transitions of $HCOOCH_3$ at 228.629 GHz and 90.146 GHz. The size of the emission region in these lines is of about 7″and 12″, respectively. Adopting these values for torsionally excited $HCOOCH_3$,

[2] A prediction of the overall spectrum of methyl formate in the ground and first excited states, on a large frequency range will be published soon (Kleiner et al. in preparation).

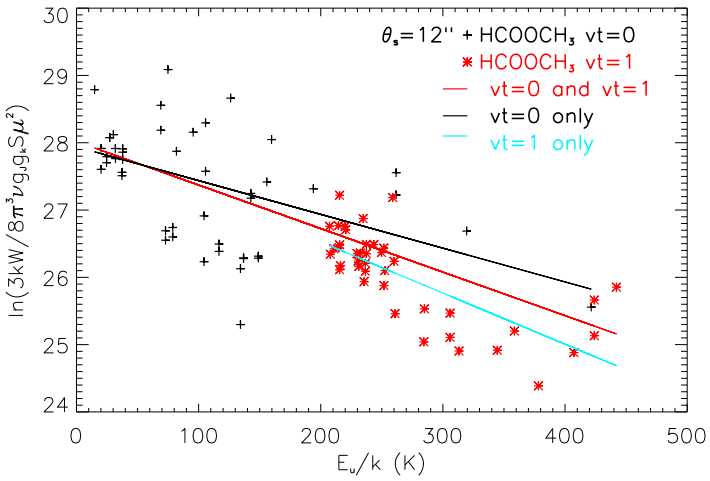

Fig. 3. Rotational diagram of methyl formate in the ground state (black crosses) and of methyl formate both in the ground and excited states (red stars). The source size is 12″. The rotational temperature and column density for methyl formate in the ground state are T_{rot} = 199 ± 28 K and N = $9.6^{+0.9}_{-0.9} \times 10^{16}$ cm^{-2} and T_{rot} = 154 ± 8 K and N = $5.6^{+4.0}_{-3.7} \times 10^{16}$ cm^{-2} when the ground and the first torsionally excited state are combined. For comparison the rotational diagram for the excited state only is plotted (blue curve).

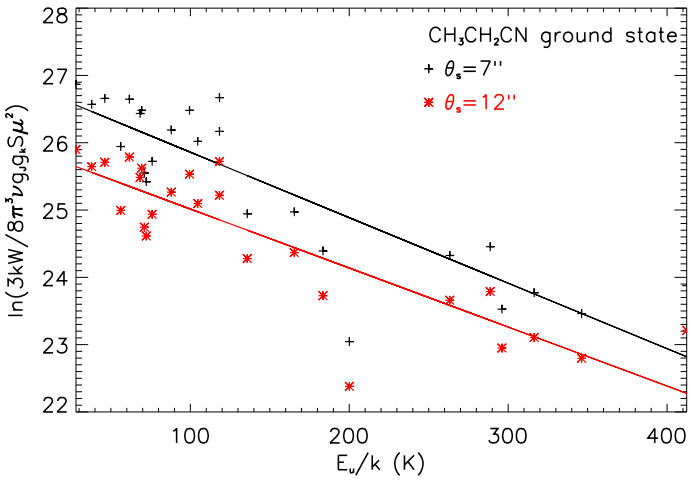

Fig. 4. Rotational diagram of the ethyl cyanide in the ground state for different source sizes. For a source size of 7″(black crosses) we find a rotational temperature of T_{rot} = 103 ± 9 K and a column density of N = $3.7^{+0.6}_{-0.5} \times 10^{15}$ cm^{-2}; for a source size of 12″(red stars) we find T_{rot} = 114 ± 11 K and N = 1.3 $\times 10^{16}$ $\times 10^{15}$ cm^{-2}.

Table 4. Temperature and column density of the detected molecules

Molecules		Source size	
		7″	12″
$HCOOCH_3$	T (K)	176 ± 24	199 ± 28
υ_t=0	N (cm^{-2})	$17.0^{+1.8}_{-1.6} \times 10^{16}$	$9.6^{+0.9}_{-0.9} \times 10^{16}$
$HCOOCH_3$	T (K)	104 ± 14	131 ± 20
υ_t=1	N (cm^{-2})	$9.4^{+4.0}_{-2.8} \times 10^{16}$	$3.4^{+1.5}_{-1.1} \times 10^{16}$
$HCOOCH_3$	T (K)	144 ± 7	154 ± 8
υ_t=0 + υ_t=1	N (cm^{-2})	$11.4^{+0.9}_{-0.8} \times 10^{16}$	$5.6^{+4.0}_{-3.7} \times 10^{16}$
CH_3CH_2CN	T (K)	103 ± 9	114 ± 11
	N (cm^{-2})	$3.7^{+0.6}_{-0.5} \times 10^{15}$	$1.7^{+0.3}_{-0.2} \times 10^{15}$

we find a rotational temperature and a column density of T_{rot} = 131 ± 20 K and N = $3.4^{+1.5}_{-1.1} \times 10^{16}$ cm^{-2} for a source size of 12″and T_{rot} = 104 ± 14 K and N = $9.4^{+4.0}_{-2.8} \times 10^{16}$ cm^{-2} for a source size of 7″(Table 4). A separate analysis of the A and E lines of excited methyl formate gives compatible values, within the uncertainty, for the rotational temperature and column density. Transitions from the ground state of $HCOOCH_3$ have been detected too. Using the rotational diagram method we find for $HCOOCH_3$ υ_t=0: T_{rot} = 199 ± 28 K and N = $9.6^{+0.9}_{-0.9} \times 10^{16}$ cm^{-2} for a 12 ″source (Fig. 3). If we consider both lines from the ground state and from υ_t=1 we find T_{rot} = 154 ± 8 K and N = $5.6^{+4.0}_{-3.7} \times 10^{16}$ cm^{-2} for a 12 ″source (Fig. 3, Table 4). These temperatures and column densities have been used to model the emission of methyl formate in the source. The comparison of the modelled spectra with the observations is shown in Fig. 1 for a number of lines from $HCOOCH_3$, υ_t=1.

5. Ethyl cyanide

Severals tens of lines from ethyl cyanide in the ground state are observed in the spectra. A large number of these lines are not blended and their energy covers a wide range, allowing to plot a rotational diagram (Fig. 4). Adopting a source size of 12″as for the ground state of methyl formate, we find a rotational temperature of T_{rot} = 114 ± 11 K and a column density N = $1.7^{+0.3}_{-0.2} \times 10^{15}$ cm^{-2}. Adopting a smaller source of 7″does not change significantly the rotational temperature but changes the column density : T_{rot} = 103 ± 9 K and a column density N = $3.7^{+0.6}_{-0.5} \times 10^{15}$ cm^{-2} (Table 4).

Ethyl cyanide appears to be colder than previously found. Liu et al. (2001) adopt a temperature of 200 K and find an abundance for this molecule of 4 × 10^{15} cm^{-2}. However their analysis is based on lines having energies lower than 113 K. If we limit ourselves to low energy transitions we find T_{rot} = 184 K and a column density N = 1.3 $\times 10^{16}$ cm^{-2}. Ikeda et al. (2001) fixed T_{rot} to 150 K and found a column density of N = 7 $\times 10^{14}$ cm^{-2}.

We have searched for transitions from the first excited bending mode (in-plane CCN bending mode) of ethyl cyanide at 206 cm^{-1} (designated by υ_b=1) and from the first torsional excited state, υ_t=1, at 212 cm^{-1}. These 2 states, together with the CCN out-of-plane bending mode at 378 cm^{-1}, have been studied by Fukuyama et al. (1999) in the 8-200 GHz range for J and $K_a \leq$ than 16 and 2, respectively. Lines from the two lowest energy states υ_b=1 and υ_t=1 have been detected toward SgrB2 by Mehringer et al. (2004). This paper presents the molecular theory used for the spectral analysis of new measurements of excited ethyl cyanide in the 85-400 GHz range for J and $K_a \leq$ than 50 and 15, respectively. However, the complete analysis has not been published yet and the prediction for the line frequencies and intensities was obtained from J. Pearson (private communication).

Most of the lines belonging to the excited states υ_t=1 and υ_b=1 are blended with other strong lines, identified or not (Table 3). However few lines allow the column density of vibrationally excited ethyl cyanide to be constrained (Table 3). We have estimated the upper limit on the abundance of ex-

cited CH_3CH_2CN by comparing the emission spectrum of excited ethyl cyanide simulated with the LTE model with the observed spectra, for different temperatures and column densities (Fig. 5). Adopting the same temperature as the ground state (100 K) and a higher temperature of 200 K we find that the column density of vibrationally excited ethyl cyanide is 10^{16}cm^{-2} and 5 $\times$ 10^{15}cm^{-2}, respectively.

6. Methyl carbamate and glycine

The initial aim of the observations was to search for methyl carbamate (NH_2COOCH_3), an isomer of glycine (NH_2CH_2COOH). Methyl carbamate has a strong dipole moment and is energetically more stable than glycine, two reasons that make it a good candidate for interstellar detection. The rotational spectrum of methyl carbamate in the A torsional substate was studied in the 8-240 GHz frequency range (Bakri et al. 2002; Ilyushin et al. 2006). This study was recently extended by Groner et al. (2007) who measured transitions of both A and E torsional substates up to 371 GHz. Our first analysis of the observations from 2003 was performed with a prediction of lines frequencies and intensities made for the A-transitions from the work from Bakri et al. (2002). We have then made a new analysis of our data from 2003 and 2006 with the predictions given by Groner et al. (2007).

Several tens of lines from methyl carbamate were searched in spectral regions carefully chosen in order to avoid or limit confusion with spectral lines from other molecules. However we did not detect methyl carbamate in our data. Furthermore, despite everything, most of the lines are fully blended and only very few lines allow us to constrain the upper limit of the abundance of methyl carbamate in W51 e2. By comparing the simulated emission spectrum of methyl carbamate at different temperatures and source sizes with the observed spectrum (Fig.6) we have constrained the upper limit of methyl carbamate in this source. For a small emission region (7″) and warm gas (200 K) we found N $\leq 5 \times 10^{14}$ cm^{-2}. This upper limit decreases as the rotational temperature and/or the size of the emission source decreases. We find N $\leq 2 \times 10^{14}$ cm^{-2} for T_{rot} = 100 K and θ_s = 12″and N $\leq 8 \times 10^{13}$ cm^{-2} for T_{rot} = 50 K and θ_s = 30″.

Numerous transitions from both conformers of glycine fall within our observed spectral ranges. Glycine is not detected in the spectra. Almost all the lines are blended and only few of them may be used to estimate roughly the upper limit of glycine in W51 e2. This upper limit varies by an order of magnitude depending on the source size, and rotational temperature. Assuming a rotational temperature of 100 K the upper limit on the column density of glycine is 3×10^{14} cm^2 for a 7″source size and 6×10^{13} cm^2 for a 30″source size.

7. Discussion

We find that the rotational temperatures derived from the rotational diagram analysis are different from the kinetic temperature, T_{kin} = 153(21) K derived by Remijan et al. (2004). The rotational temperature of ethyl cyanide (103 - 114 K) is lower than T_{kin} independently of the adopted source size. It is higher than T_{kin} if we consider methyl formate in its ground state (176 - 199 K), lower if we consider only the excited state (104 - 131 K) and of the same order if we consider simultaneously the ground state and the first excited state of methyl formate (144 -154 K). All this tends to indicates that the LTE hypothesis is probably not fully valid. However, despite these possible departure from LTE, the rotational diagram method which implicitly assume that LTE is reached and that all temperature are equivalent (i.e. $T_{exc} = T_{kin} = T_{rot} = T_{vib}$), is the only one left for us to get an estimation of the excitation temperature since a statistical analysis is ruled out by the absence of known collision rates for the studied molecules.

The relevance of the LTE assumption within each rotational level may also be evaluated by comparing the cloud density to the critical density of each vibrational state. Collisional rates are not known for molecules as complex as methyl formate or ethyl cyanide. However, it is possible to estimate roughly the critical density for these molecules by adopting the value of methanol interacting with H_2, of the order of a few 10^{-11} cm^3.s^{-1} (Pottage et al. 2004) and assuming it is the same for the ground and vibrational excited states. The Einstein coefficients of the rotational transitions are in the range 10^{-5}-10^{-6} s^{-1}. The critical density is thus of the order of 10^5-10^6 cm^{-3}, i.e., comparable to the hydrogen density in W51 e2 estimated to be n_H = 5(2) $\times$ 10^5 cm^{-3} (Remijan et al. 2004). There is thus a competition between collisional and radiative excitation and it is clear that the levels are probably not all thermalized.

The excitation mechanism populating the observed excited state of methyl formate and ethyl cyanide may be infered in a similar way. The Einstein coefficients for ro-vibrational transitions from the excited states to the ground state are of the order of a few 10^{-1} s^{-1}, much greater than for rotational transitions within the excited state (10^{-5}-10^{-6} s^{-1}). Thus, adopting the same value for the collisional rate as before (a few 10^{-11} cm^3.s^{-1}), the density needed to thermalize the levels in the excited state by collisions must be greater than the critical density which is of the order of 10^{10} cm^{-3}. The dust in W51 e2 has a temperature of about 140 K (Sollins et al. 2004) and thus emits efficiently at the wavelength of the excited states of both molecules. It is thus most probable that the excited states of methyl formate and ethyl cyanide are populated by radiative processes rather than by collisions.

We find that the rotational temperature of the gas decreases when the source size gets smaller. This is surprising since it is expected that the deepest regions of hot cores are also the warmest. The observed transitions are optically thin for the adopted source sizes of 12″and 7 ″. BIMA observations of methyl formate in W51 e2 (Remijan et al. 2002) show that the emission region is smaller for high energy transition than for low energy transition. The size of the emission region is around 12″for the $7_{2,5}$-$6_{2,4}$ transition at 90146 MHz corresponding to an energy of 10 cm^{-1} (15 K) and around 7″for the $18_{5,13}$-$17_{5,12}$ transition at 228629 MHz corresponding to an energy of 75 cm^{-1} (108 K). More interferometric observations are needed to locate precisely the emission region of methyl formate and ethyl cyanide in the ground and excited state and understand their temperature distribution.

The presence of methyl formate in torsional excited state in hot cores such as W51 e2 and Orion KL (Kobayashi et al. 2007) is not surprising. Methyl formate is very abundant and its torsional mode has a very low energy (188 K). By comparison, it is not surprising that ethyl cyanide is more difficult to detect: it is less abundant and its excited states lie at slightly higher energy, around 300 K. However it is clear that observations having better signal to noise, better spectral and angular resolution, such as forthcoming observations from Herschel and ALMA, will reveal much more lines from excited states of these molecules

but also of abundant large molecules possessing low-frequency vibrational states. For example dimethyl ether, CH_3OCH_3, has two torsional modes at about 203 and 242 cm^{-1} and transitions from these modes should be present in the spectra of hot cores. More generally, a large number of unidentified lines reported in the spectra of hot molecular clouds should be due to transitions from abundant molecules in excited states.

Acknowledgements. The authors would like to thank Alexandre Faure for fruitful discussions, Jean Demaison and Isabelle Kleiner for invaluable help in the methyl formate study and John Pearson for providing us with the excited ethyl cyanide spectrum. We acknowledge all the Pico Veleta IRAM staff for their help during the observations. We thank the referee for his/her constructive comments. This work was supported by the Programme National "Physico Chimie du Milieu Interstellaire" and by the European Research Training Network "Molecular Universe" (MRTN-CT-2004-512302). M.C. thanks the CNRS (project CERC3) and Junta de Andalucia (project P07-FQM-03014) for financial support.

References

Bakri, B., Demaison, J., Kleiner, I., et al. 2002, Journal of Molecular Spectroscopy, 215, 312
Carvajal, M., Willaert, F., Demaison, J., & Kleiner, I. 2007, Journal of Molecular Spectroscopy, 246, 158
Demaison, J., Boucher, D., & Dubrulle, A. 1984, Journal of Molecular Spectroscopy, 102, 260
Fuchs, G. W., Fuchs, U., Giesen, T. F., & Wyrowski, F. 2005, A&A, 444, 521
Fukuyama, Y., Omori, K., Odashima, H., Takagi, K., & Tsunekawa, S. 1999, Journal of Molecular Spectroscopy, 193, 72
Gordy, W. & Cook, R. L. 1984, Microwave Molecular Spectra (New York: John Wiley & Sons)
Groner, P., Winnewisser, M., Medvedev, I. R., et al. 2007, ApJS, 169, 28
Hollis, J. M., Lovas, F. J., Remijan, A. J., et al. 2006, ApJ, 643, L25
Hougen, J. T., Kleiner, I., & Godefroid, M. 1994, Journal of Molecular Spectroscopy, 163, 559
Ikeda, M., Ohishi, M., Nummelin, A., et al. 2001, ApJ, 560, 792
Ilyushin, V., Alekseev, E., Demaison, J., & Kleiner, I. 2006, Journal of Molecular Spectroscopy, 240, 127
Ilyushin, V., Kleiner, I., & Lovas, F. J. 2007, Journal of Physical and Chemical Reference Data
Kleiner, I., Lovas, F. J., & Godefroid, M. 1996, Journal of Physical and Chemical Reference Data, 25, 1113
Kobayashi, K., Ogata, K., Tsunekawa, S., & Takano, S. 2007, ApJ, 657, L17
Liu, S.-Y., Mehringer, D. M., & Snyder, L. E. 2001, ApJ, 552, 654
Mehringer, D. M., Pearson, J. C., Keene, J., & Phillips, T. G. 2004, ApJ, 608, 306
Nummelin, A., Bergman, P., Hjalmarson, A., et al. 1998, ApJS, 117, 427
Oesterling, L. C., Albert, S., De Lucia, F. C., Sastry, K. V. L. N., & Herbst, E. 1999, ApJ, 521, 255
Ogata, K., Odashima, H., Takagi, K., & Tsunekawa, S. 2004, Journal of Molecular Spectroscopy, 225, 14
Plummer, G. M., Herbst, E., De Lucia, F., & Blake, G. A. 1984, ApJS, 55, 633
Plummer, G. M., Herbst, E., De Lucia, F. C., & Blake, G. A. 1986, ApJS, 60, 949
Pottage, J. T., Flower, D. R., & Davis, S. L. 2004, MNRAS, 352, 39
Remijan, A., Snyder, L. E., Liu, S.-Y., Mehringer, D., & Kuan, Y.-J. 2002, ApJ, 576, 264
Remijan, A., Sutton, E. C., Snyder, L. E., et al. 2004, ApJ, 606, 917
Snyder, L. E., Lovas, F. J., Hollis, J. M., et al. 2005, ApJ, 619, 914
Sollins, P. K., Zhang, Q., & Ho, P. T. P. 2004, ApJ, 606, 943
Turner, B. E. 1991, ApJS, 76, 617
Zhang, Q., Ho, P. T. P., & Ohashi, N. 1998, ApJ, 494, 636

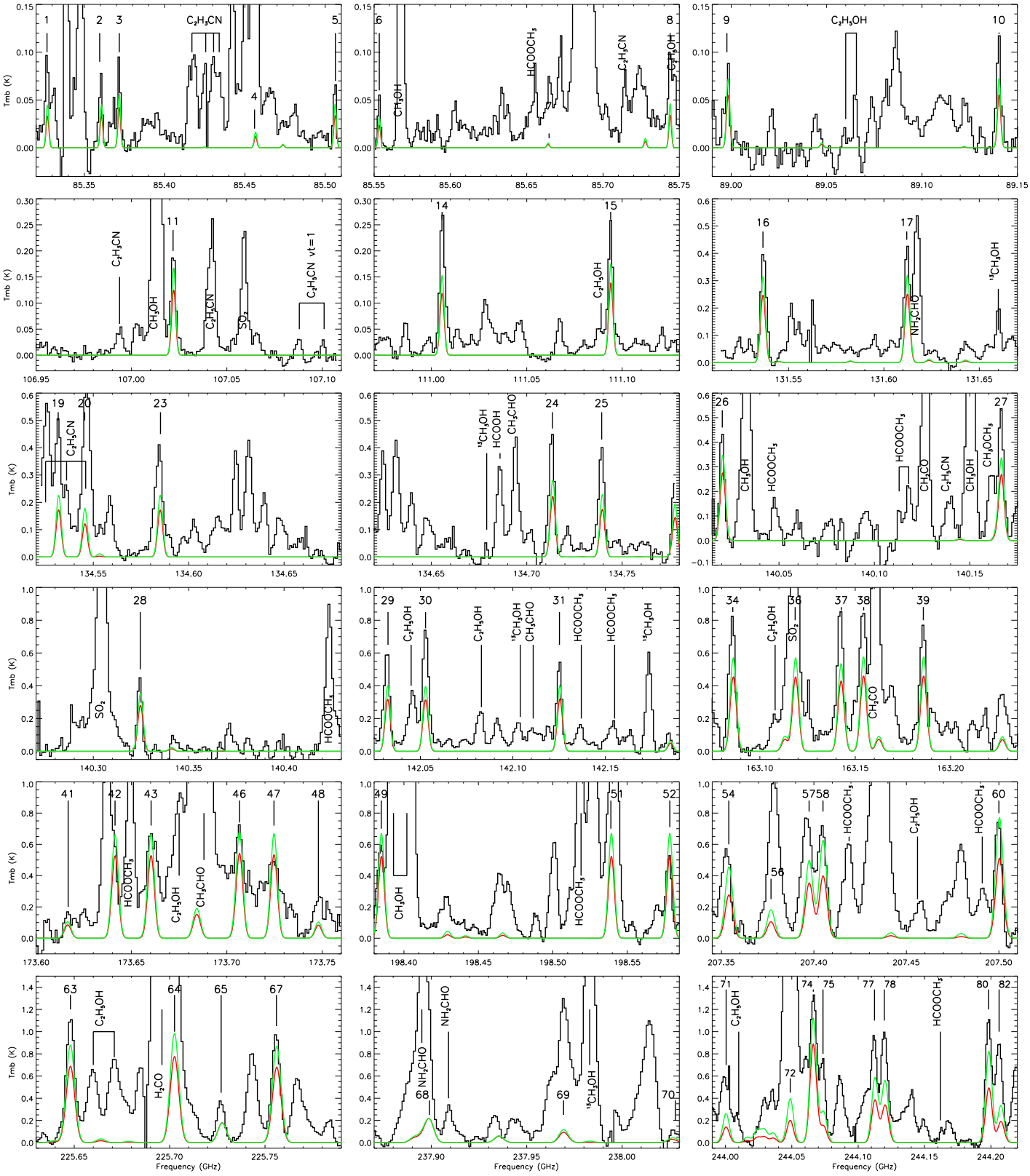

Fig. 1. Detected lines from the first torsionally excited state of methyl formate $HCOOCH_3$. The observations (histogram like curve) are compared with LTE emission models of $HCOOCH_3$ $\upsilon_t = 1$with $\theta_s = 7''$, T_{rot} = 104 K and N = 9.4 $\times 10^{16}$ cm^{-2} (red curve) and with θ_s = 12", T_{rot} = 154 K and N = 5.6 $\times$ 10^{16} cm^{-2} (green curve). The numbered lines are transitions from torsionally excited $HCOOCH_3$, see Table 2 for the attribution of each line.

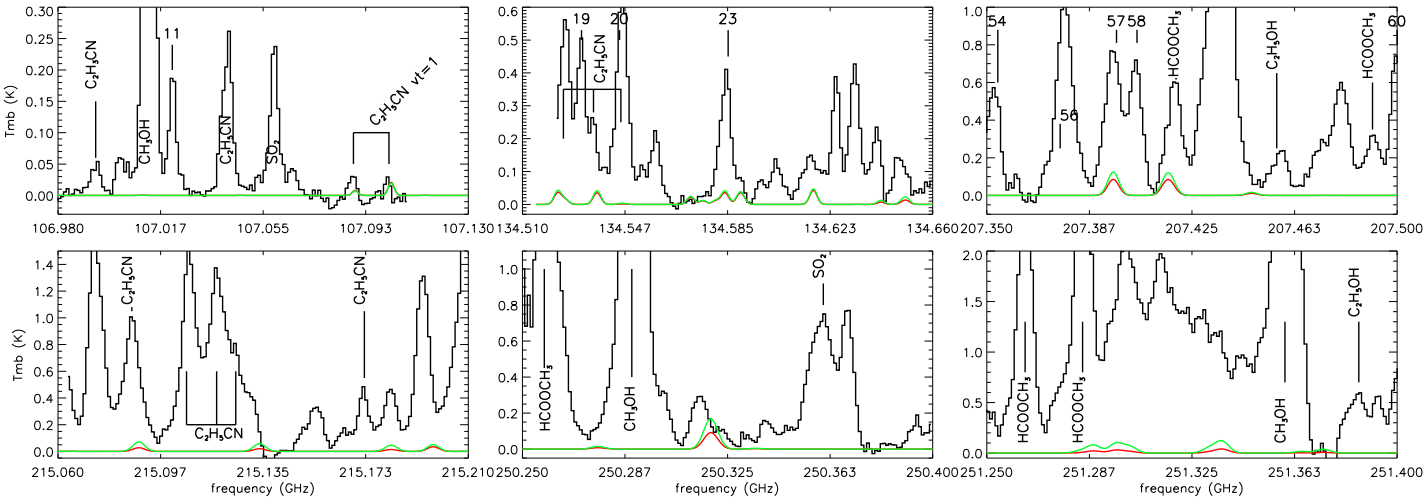

Fig. 5. Detected lines from the first two excited states υ_t=1 and υ_b=1 of ethyl cyanide CH_3CH_2CN. The observations (histogram like curve) are compared with LTE emission models of CH_3CH_2CN υ_t=1 and υ_b=1 with θ_s = 7", T =100 K and N = 10^{16} cm^{-2} (red curve) and T = 200 K and N = 5×10^{15} cm^{-2} (green curve). The numbered lines are excited methyl formate lines (see Table 2). See Table 3 for the identification of the excited CH_3CH_2CN lines.

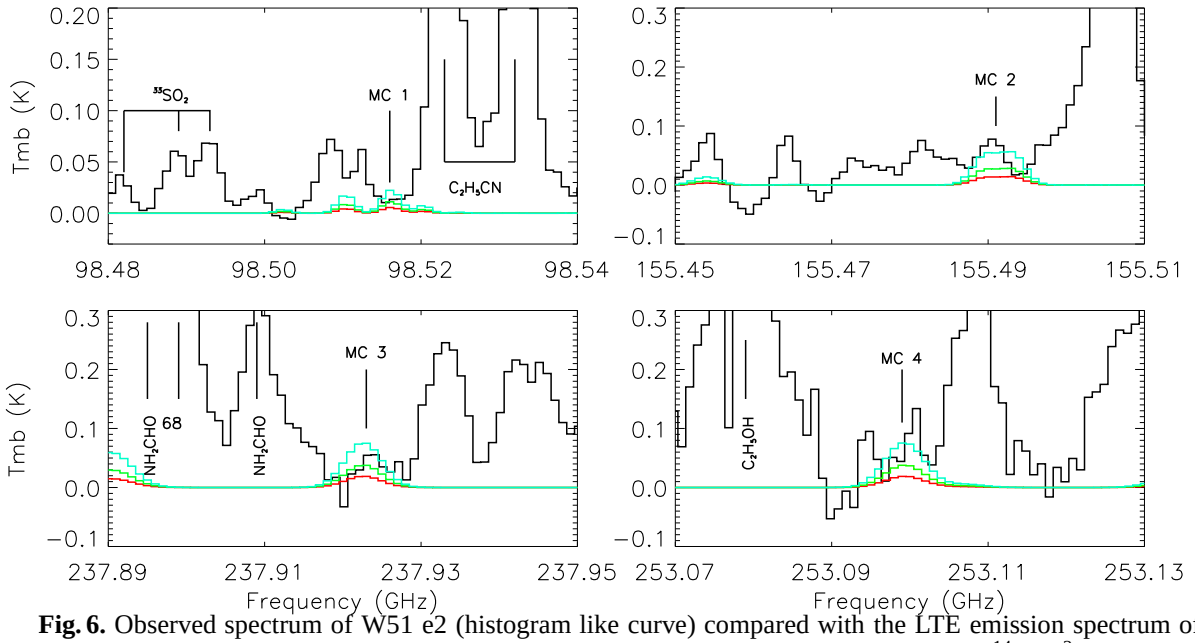

Fig. 6. Observed spectrum of W51 e2 (histogram like curve) compared with the LTE emission spectrum of methyl carbamate at different densities, for a 12″source and rotational temperature of 100 K: red curve: N = 10^{14} cm^{-2}, green curve: N = 2×10^{14} cm^{-2}, blue curve: N = 4×10^{14} cm^{-2}. The methyl carbamate lines are (from Groner et al. 2007): MC1 : $14_{2,13} - 13_{1,12}$ (E) at 98515.38 GHz and $15_{1,15} - 14_{0,14}$ E and A at 98516.99 GHz; MC2 : $23_{1,22} - 22_{2,21}$ at 155489.10 and 155492.68 GHz for the E and A symmetry, respectively and $23_{2,22} - 22_{1,21}$ at 155490.07 and 155493.65 GHz for the E and A symmetry, respectively; MC3 : $14_{10,5} - 13_{9,4}$ (A) and $14_{10,4} - 13_{9,5}$ (A) (blended) at 237922.60 GHz; MC4 : $16_{10,7} - 15_{9,6}$ (A) and $16_{10,6} - 15_{9,7}$ (A) at 253099.30 and 253099.37 GHz, respectively.

Table 1. Laboratory measurements, calculated frequencies and line strengths for methyformate transitions in the first torsionally excited state used in the present detection.

J'	K_a'	K_c'	P'	J"	K_a"	K_c"	P"	Obs. Freq	Calc.Freq	Calc.Unc	Obs-Calc	$S\mu^2$	E_l
Upper State[a]				Lower State[a]				(MHz)[b]	(MHz)[c]	(kHz)[c]	(MHz)[c]	(D^2)	(cm^{-1})[d]
7	4	4	-	6	4	3	-	85327.104	85327.085	11	0.019	12.483	146.8606
7	4	3	+	6	4	2	+	85360.669	85360.823	11	-0.154	12.483	146.8610
7	3	5	+	6	3	4	+	85371.762	85371.789	11	-0.027	15.120	143.6253
7	-6	2		6	-6	1			85456.630	19		4.944	155.5393
7	4	3		6	4	2		85506.175	85506.179	16	-0.004	12.571	146.6097
7	-5	3		6	-5	2		85553.365	85553.288	17	0.077	9.123	150.4139
10	2	9	-	10	1	10	+	85664.038	85663.943	20	0.095	1.403	151.8343
11	4	7	+	11	3	8	-	85727.753	85727.728	18	0.025	3.078	162.4132
7	-4	4		6	-4	3		85743.967	85743.894	16	0.073	12.532	146.2356
7	2	5	+	6	2	4	+	88998.368	88998.415	12	-0.047	17.049	141.4958
7	2	5		6	2	4		89140.383	89140.366	18	0.017	17.051	141.0232
25	5	20	-	25	4	21	+		107021.644	361		8.289	274.8357
9	-2	8		8	-2	7		107022.162	107022.092	13	0.070	22.628	146.6924
10	1	9	-	9	2	8	-	107472.351	107472.387	15	-0.036	2.144	150.7587
9	-3	7		8	-3	6		111005.617	111005.582	19	0.035	20.800	149.1777
9	1	8		8	1	7		111094.105	111094.056	13	0.049	23.222	146.0900
12	0	12	+	11	0	11	+	131536.624	131536.653	12	-0.029	31.375	155.8502
12	0	12		11	0	11		131612.344	131612.301	13	0.043	31.558	155.3072
12	1	12	+	11	0	11	+	131764.316	131764.341	12	-0.025	4.870	155.8502
11	5	7	+	10	5	6	+	134531.846	134531.833	13	0.013	23.125	164.8530
27	7	20	-	27	6	21	+		134545.609	582		8.581	304.5077
11	-7	5		10	-7	4		134545.615	134545.516	27	0.099	17.431	175.4588
35	8	27	+	35	7	28	-		134553.290	912		12.622	416.6235
11	5	6	-	10	5	5	-	134585.070	134585.141	13	-0.071	23.125	164.8541
11	-3	9		10	-3	8		134713.629	134713.526	16	0.103	26.708	156.9827
11	5	6		10	5	5		134739.630	134739.629	19	0.001	23.251	164.7142
12	2	11	-	11	2	10	-	140020.525	140020.564	12	-0.039	30.616	158.9957
11	2	9	+	10	2	8	+	140166.667	140166.713	12	-0.046	28.103	155.9781
12	-2	11		11	-2	10		140324.728	140324.699	12	0.029	30.787	158.5211
13	-1	13		12	-1	12		142032.334	142032.293	14	0.041	34.222	159.7047
13	0	13	+	12	0	12	+	142052.800	142052.735	14	0.065	34.029	160.2378
13	0	13		12	0	12		142125.416	142125.410	14	0.006	34.224	159.6973
13	1	13	+	12	0	12	+	142185.220	142185.198	14	0.022	5.339	160.2378
15	0	15	+	14	1	14	+	163042.398	163042.248	20	0.100	6.267	170.0683
15	1	15	+	14	1	14	+	163086.032	163085.873	20	0.159	39.344	170.0683
15	0	15		14	-1	14		163113.094	163113.156	18	-0.062	6.073	169.5325
15	0	15	+	14	0	14	+	163118.722	163118.574	20	0.148	39.345	170.0657
14	1	13		13	1	12		163142.587	163142.607	14	-0.020	36.185	168.1362
15	-1	15		14	-1	14		163154.325	163154.404	18	-0.079	39.561	169.5325
15	0	15		14	0	14		163185.864	163185.922	18	-0.058	39.561	169.5300
15	-1	15		14	0	14		163227.097	163227.169	18	-0.072	6.074	169.5300
16	0	16	+	15	1	15	+	173616.616	173616.407	25	0.209	6.727	175.5082
16	1	16	+	15	1	15	+	173641.411	173641.171	25	0.240	42.007	175.5082
16	0	16	+	15	0	15	+	173660.281	173660.032	25	0.249	42.007	175.5068
16	0	16		15	-1	15		173683.479	173683.597	23	-0.118	6.525	174.9747
24	3	21	-	24	2	22	+		173704.470	241		4.324	254.0651
16	-1	16		15	-1	15		173706.683	173706.807	23	-0.124	42.232	174.9747
16	0	16		15	0	15		173724.731	173724.845	23	-0.114	42.232	174.9733
16	-1	16		15	0	15		173747.990	173748.055	23	-0.065	6.525	174.9733
16	5	11		15	5	10		198384.885	198384.966	32	-0.081	38.205	191.3885
26	8	19	-	26	7	20	+		198429.332	290		6.921	297.4256
16	5	11	-	15	5	10	-		198539.350	30		38.279	191.5148
16	-5	12		15	-5	11		198578.563	198578.589	33	-0.026	38.090	191.0593
19	3	16	-	18	4	15	-		207295.959	118		2.804	208.1331
17	12	5	+	16	12	4	+		207354.058	101		12.640	252.9573
17	12	6	-	16	12	5	-		207354.058	101		12.640	252.9573
17	-13	5		16	-13	4			207376.777	145		18.783	264.5661
17	9	8		16	9	7			207397.312	68		32.511	223.9160

continued on next page

Table 1. Laboratory measurements, calculated frequencies and line strengths for methyformate transitions in the first torsionally excited state used in the present detection. – continued from previous page

J'	K_a'	K_c'	P'	J"	K_a"	K_c"	P"	Obs. Freq (MHz)[b]	Calc.Freq (MHz)[c]	Calc.Unc (kHz)[c]	Obs-Calc (MHz)[c]	$S\mu^2$ (D^2)	E_l (cm^{-1})[d]
Upper State[a]				Lower State[a]									
17	11	7	+	16	11	6	+		207404.993	81		26.248	242.2767
17	11	6	-	16	11	5	-		207404.993	81		26.248	242.2767
17	10	8	-	16	10	7	-		207500.297	66		29.526	232.5324
17	10	7	+	16	10	6	+		207500.297	66		29.526	232.5324
19	2	18	-	18	1	17	-		215130.469	47		6.562	199.2115
18	5	13	-	17	5	12	-		225648.010	57		44.072	205.2072
19	2	17	+	18	2	16	+		225702.569	46		48.659	203.7419
6	6	1	-	5	5	0	-		225727.540	30		2.592	148.5921
6	6	0	+	5	5	1	+		225727.552	30		2.592	148.5921
18	5	13		17	5	12			225756.154	54		43.428	205.0713
7	6	1	+	6	5	2	+		237899.077	27		2.594	151.0254
20	3	18	+	19	2	17	+		237969.273	58		5.371	211.2706
37	7	31	+	37	6	32	-		238027.934	1642		8.537	434.5487
20	-14	7		19	-14	6			244000.464	195		27.134	299.1664
20	15	5	-	19	15	4	-		244048.806	207		23.017	312.5791
20	15	6	+	19	15	5	+		244048.806	207		23.017	312.5791
19	4	15	+	18	4	14	+		244066.113	79		48.355	209.5678
27	1	26	-	27	0	27	+		244066.575	470		1.456	268.2307
20	14	6	+	19	14	5	+		244073.956	178		20.522	299.0954
20	14	7	-	19	14	6	-		244073.956	178		20.522	299.0954
20	10	10		19	10	9			244112.669	108		39.852	254.7516
20	13	7	-	19	13	6	-		244119.960	154		24.670	286.5471
20	13	8	+	19	13	7	+		244119.960	154		24.670	286.5471
20	12	8	+	19	12	7	+		244198.512	134		34.020	274.9352
20	12	9	-	19	12	8	-		244198.512	134		34.020	274.9352
20	-13	8		19	-13	7			244207.619	159		30.739	286.5459

[a]Upper and lower state transitions quantum numbers. The rotational quantum number J, and the asymmetric rotor labels K_a and K_c are identified for each energy level. For the A symmetry species, P is the parity quantum number, for the E species, P is not defined, instead, the K_a label has a signed value (Hougen et al. 1994; Ilyushin et al. 2007). Note that this information has been suppressed in Table 2, otherwise the quantum number labeling is the same.
[b]Observed laboratory frequencies in MHz from Ogata et al. (2004), the experimental uncertainty is 50 kHz for all measured lines.
[c]Calculated frequencies, uncertainties and obs-calc values are from (Carvajal et al. 2007) for the measured lines, the predicted frequencies and uncertainties for unmeasured lines is from Kleiner et al. (private communication).
[d]Lower state energy in cm^{-1}, relative to the J=K=0 A species levels, set as zero energy.

Table 2. Detected transitions of the first torsionally excited state of $HCOOCH_3$ in W51 e2.

	Transition[a]	$S\mu^2$ (D^2)	E_l (cm^{-1})	Frequency (MHz)	Obs. frequency[b] (MHz)	$\int T_{mb}\Delta v$[c] ($K.km.s^{-1}$)	T_{mb} (mK)	Comment[d]
1(8)	7(4,4) - 6(4,3) A	12.5	146.86	85327.104	85326.864	1.22	87	
2(5)	7(4,3) - 6(4,2) A	12.5	146.86	85360.669	85359.685	0.40	81	
3	7(3,5) - 6(3,4) A	15.1	143.62	85371.762	85371.871	0.67	102	
4	7(6,2) - 6(6,1) E	4.94	155.53	85456.630	85456.067	14.33	1133	CH_3CCH
5(2)	7(4,3) - 6(4,2) E	12.6	146.60	85506.175	85506.053	0.57	84	
6	7(5,3) - 6(5,2) E	9.12	150.40	85553.365	85553.361	0.54	78	
7	10(2,9) - 10(1,10) A	1.40	151.83	85664.038	85664.621	1.06	61	C_2H_3CN
8(1)	7(4,4) - 6(4,3) E	12.5	146.22	85743.967	85743.915	0.79	102	
9(10)	7(2,5) - 6(2,4) A	17.0	141.50	88998.368	88997.692	0.77	83	
10(9)	7(2,5) - 6(2,4) E	17.1	141.01	89140.383	89140.161	1.20	120	
11	25(5,20) - 25(4,21) A	8.29	274.84	107021.644	107021.862	1.99	186	
12	9(2,8) - 8(2,7) E	22.6	146.68	107022.162	-	-	-	
13	10(1,9) - 9(2,8) A	2.14	150.76	107472.351	107472.400	0.27	45	
14	9(3,7) - 8(3,6) E	20.8	149.16	111005.617	111005.832	2.67	261	
15	9(1,8) - 8(1,7) E	23.2	146.08	111094.105	111094.010	2.27	244	
16(17)	12(0,12) - 11(0,11) A	31.4	155.85	131536.624	131536.949	3.53	407	
17(16)	12(0,12) - 11(0,11) E	31.6	155.29	131612.344	131612.094	3.97	410	
18	12(1,12) - 11(0,11) A	4.87	155.85	131764.316	131765.100	1.70	100	$S^{18}O$
19	11(5,7) - 10(5,6) A	23.1	164.85	134531.846	134531.411	3.44	478	SO_2 υ_2=1
20	27(7,20) - 27(6,21) A	8.58	304.51	134545.609	134546.431	7.95	630	C_3H_2CN + $^{33}SO_2$
21	11(7,5) - 10(7,4) E	17.4	175.45	134545.615	-	-	-	-
22	35(8,27) - 35(7,28) A	12.6	416.62	134553.290	134553.647	0.71	991	$^{33}SO_2$
23(25)	11(5,6), - 10(5,5) A	23.1	164.85	134585.070	134584.263	4.68	382	$C_3H_2CN\upsilon_t$,υ_b=1 and ?
24	11(3,9) - 10(3,8) E	26.7	156.97	134713.629	134713.062	3.59	456	
25(23)	11(5,6) - 10(5,5) E	23.3	164.70	134739.630	134739.110	3.55	386	
26(28)	12(2,11) - 11(2,10) A	30.6	159.00	140020.525	140020.145	2.96	472	
27	11(2,9) - 10(2,8) A	28.1	155.98	140166.667	140166.502	3.42	528	
28(26)	12(2,11) - 11(2,10) E	30.8	158.50	140324.728	140324.321	7.66	470	
29	13(1,13) - 12(1,12) E	34.2	159.69	142032.334	142031.811	4.52	586	
30(31)	13(0,13) - 12(0,12) A	34.0	160.24	142052.800	142052.867	5.95	724	
31(30)	13(0,13) - 12(0,12) E	34.2	159.68	142125.416	142125.086	4.01	559	
32	13(1,13) - 12(0,12) A	5.34	160.24	142185.220	142184.202	0.81	121	
33(35)	15(0,15) - 14(1,14) A	6.27	170.07	163042.398	163042.050	2.32	363	
34(38)	15(1,15) - 14(1,14) A	39.3	170.07	163086.032	163085.494	6.39	884	$HCOOCH_3$ υ_t=0
35(33)	15(0,15) - 14(1,14) E	6.07	169.52	163113.094	163113.656	5.11	549	SO_2
36(39)	15(0,15) - 14(0,14) A	39.3	169.52	163118.722	163118.285	19.40	2184	SO_2
37	14(1,13) - 13(1,12) E	36.2	168.12	163142.587	163141.991	7.69	967	
38(34)	15(1,15) - 14(1,14) E	39.6	162.52	163154.325	163153.604	8.99	855	
39(36)	15(0,15) - 14(0,14) E	39.6	169.52	163185.864	163185.586	5.15	679	
40	15(1,15) - 14(0,14) E	6.07	169.52	163227.097	163227.290	4.23	448	
41(44)	16(0,16) - 15(1,15) A	6.73	175.51	173616.616	173617.000	1.80	177	
42(46)	16(1,16) - 15(1,15) A	42.0	175.51	173641.411	173636.978	15.14	1288	$HCOOCH_3$ υ_t=0
43(47)	16(0,16) - 15(0,15) A	42.0	175.51	173660.281	173659.384	4.12	380	
44(41)	16(0,16) - 15(1,15) E	6.50	175.51	173683.479	173186.987	17.8	5300	CH_3CHO
45	24(3,21) - 24(2,22) A	4.32	254.06	173704.470	173706.183	9.03	644	
46(42)	16(1,16) - 15(1,15) E	42.2	174.96	173706.683	173706.183	-	-	
47(43)	16(0,16) - 15(0,15) E	42.2	174.97	173724.731	173724.558	2.02	479	
48	16(1,16) - 15(0,15) E	6.6	174.97	173747.990	173748.150	3.94	264	
49(51)	16(5,11) - 15(5,10) E	38.2	191.37	198384.885	198384.516	5.23	467	
50	26(8,19) - 26(7,20) A	6.92	297.43	198429.332	198428.202	1.67	231	c-C_2H_4
51(49)	16(5,11) - 15(5,10) A	38.3	191.52	198539.350	198541.500	19.44	1400	$HCOOCH_3$ υ_t=0
52	16(5,12) - 15(5,11) E	38.1	191.05	198578.563	198577.928	3.20	484	
53	19(3,16) - 18(4,15) A	2.8	208.13	207295.959	207296.361	5.16	159	CH_3CH_2CN
54	17(12,5) - 16(12,4) A	21.2	252.96	207354.058	207352.197	5.57	557	
55	17(12,6) - 16(12,5) A	21.2	252.96	-	-	-	-	
56	17(13,5) - 16(13,4) E	18.8	264.55	207376.777	207378.506	11.46	995	CH_2NH
57	17(9,8) - 16(9,7) E	32.5	223.90	207397.312	207396.134	8.62	758	
58	17(11,6) - 16(11,5) A	26.2	242.28	207404.993	207404.612	5.67	690	
59	17(11,7) - 16(11,6) A	26.2	242.28	-	-	-	-	
60	17(10,8) - 16(10,7) A	29.5	232.53	207500.297	207499.521	4.8	897	
61	17(10,7) - 16(10,6) A	29.5	232.53	-	-	-	-	
62	19(2,18) - 18(1,17) A	6.56	199.21	215130.469	215130.828	2.59	394	CH_3CH_2CN
63(67)	18(5,13) - 17(5,12) A	44.1	205.21	225648.010	225647.974	5.16	1103	$HCOOCH_3$ υ_t=0
64	19(2,17) - 18(2,16) A	48.7	203.74	225702.569	225698.559	184	1400	H_2CO
65	6(6,1) - 5(5,0) A	2.59	148.59	225727.540	225726.732	2.55	372	CH_2DCN

continued on next page

Table 2. Detected transitions of $HCOOCH_3$ υ_t=1 in W51 e2 – continued from previous page

	Transition[a]	$S\mu^2$ (D^2)	E_l (cm^{-1})	Frequency (MHz)	Obs. frequency[b] (MHz)	$\int T_{mb}\Delta v$[c] ($K.km.s^{-1}$)	T_{mb} (mK)	Comment[d]
66	6(6,0) - 5(5,1) A	2.59	148.59	225727.552	-	-	-	-
67(63)	18(5,13) - 17(5,12) E	43.4	205.06	225756.154	225755.178	7.3	927	
68	7(6,1) - 6(5,2) A	25.6	229.84	237899.08	237896.263	15.91	1.667	NH_2CHO
69	20(3,18) - 19(2,17) A	5.37	211.27	237969.273	237969.938	12.80	1.186	unidentified species
70	37(7,31) - 37(6,32) A	8.54	434.55	238027.934	238026.742	1.12	122	
71	20(14,7) - 19(14,6) E	27.1	299.15	244000.464	243999.803	7.82	596	
72	20(15,6) - 19(15,5) A	23.3	312.58	244048.806	244048.230	90.33	10.84	H_2CS
73	20(15,5) - 19(15,4) A	23.3	312.58	-	-	-	-	-
74	19(4,15) - 18(4,14) A	18.4	209.57	244066.113	244066.720	5.49	730	
75	20(14,7) - 19(14,6) A	14.2	299.10	244073.956	244073.440	3.54	314	unidentified species
76	20(14,6) - 19(14,5) A	14.2	299.10	-	-	-	-	
77	20(10,10) - 19(10,9) E	39.9	254.74	244112.669	244112.254	2.65	677	
78(82)	20(13,8) - 19(13,7) A	21.0	286.55	244119.960	244119.708	2.95	886	
79	20(13,7) - 19(13,6) A	21.0	286.55	-	-	-	-	
80	20(12,8) - 19(12,7) A	34.0	274.94	244198.512	244198.232	7.43	1107	
81	20(12,9) - 19(12,8) A	34.0	274.94	-	-	-	-	
82(78)	20(13,8) - 19(13,7) E	30.7	286.54	244207.619	244206.113	7.33	893	unidentified species

[a]The notation for the quantum numbers is the same as Table 1 except that it does not contain information on the parity of the level, i.e. the signs present in Table 1 (associated to K_a for the E species and in a separate column for the A species) have been suppressed.
[b]Observed frequencies for a systemic velocity of V_{lsr} = 55.3 $km.s^{-1}$.
[c]The line width is of the order of 7-8 $km.s^{-1}$.
[d]This column indicates the molecules blended with the detected $HCOOCH_3$ υ_t=1 transitions.
The dashes indicates that the value is the same as the one in the previous line.

Table 3. Detected transitions of excited CH_3CH_2CN ($\upsilon_b = 1$ and $\upsilon_t = 1$) in W51 e2.

Transition	State	$S\mu^2$ (D^2)	E_l (cm^{-1})	Frequency (MHz)	Obs. frequency[a] (MHz)	$\int T_{mb}\Delta v$[b] ($K.km.s^{-1}$)	T_{mb} (mK)	Comment
$11_{8,4} - 10_{8,3}$	$\upsilon_t = 1E$	116.0	281.68	98463.46	98462.15	0.82	62	
$11_{8,3} - 10_{8,2}$	$\upsilon_t = 1E$	-	-	98464.02	-	-	-	
$11_{8,4} - 10_{8,2}$	$\upsilon_t = 1A$	-	-	98464.27	-	-	-	
$11_{8,3} - 10_{8,3}$	$\upsilon_t = 1A$	-	-	98464.32	-	-	-	
$11_{9,3} - 10_{9,2}$	$\upsilon_t = 1E$	79.2	295.40	98538.53	98537.9	(c)	≤ 15	CH_3CH_2CN
$11_{9,2} - 10_{9,1}$	$\upsilon_t = 1E$	-	-	98538.84	-	-	-	-
$11_{9,3} - 10_{9,1}$	$\upsilon_t = 1A$	-	-	98539.10	-	-	-	-
$11_{9,2} - 10_{9,2}$	$\upsilon_t = 1A$	-	-	98539.11	-	-	-	-
$11_{7,4} - 10_{7,3}$	$\upsilon_b = 1E$	156.3	258.45	98556.61	98557.5	(c)	≤ 50	(c)
$11_{7,5} - 10_{7,4}$	$\upsilon_b = 1E$	-	-	98556.88	-	-	-	-
$11_{7,5} - 10_{7,3}$	$\upsilon_b = 1A$	-	-	98557.12	-	-	-	-
$11_{7,4} - 10_{7,4}$	$\upsilon_b = 1A$	-	-	98557.27	-	-	-	-
$11_{6,6} - 10_{6,5}$	$\upsilon_b = 1E$	188.1	248.92	98617.87	98619.1	2.2	105	(d)
$11_{6,5} - 10_{6,4}$	$\upsilon_b = 1E$	-	-	98617.91	-	-	-	-
$11_{6,6} - 10_{6,4}$	$\upsilon_b = 1A$	-	-	98618.09	-	-	-	-
$11_{6,5} - 10_{6,5}$	$\upsilon_b = 1A$	-	-	98618.19	-	-	-	-
$11_{4,8} - 10_{4,7}$	$\upsilon_t = 1A$	237.0	242.51	98619.45	-	-	-	-
$11_{5,7} - 10_{5,5}$	$\upsilon_t = 1A$	199.0	249.94	98620.23	-	-	-	-
$11_{5,6} - 10_{5,6}$	$\upsilon_t = 1A$	-	-	98620.33	-	-	-	-
$11_{4,8} - 10_{4,7}$	$\upsilon_t = 1E$	237.0	242.51	98620.38	-	-	-	-
$11_{5,7} - 10_{5,6}$	$\upsilon_t = 1E$	212.8	249.94	98620.41	-	-	-	-
$11_{4,7} - 10_{4,6}$	$\upsilon_t = 1A$	237.0	242.51	98620.80	-	-	-	-
$11_{4,7} - 10_{4,6}$	$\upsilon_t = 1E$	-	-	98620.82	-	-	-	-
$11_{5,6} - 10_{5,5}$	$\upsilon_t = 1E$	212.8	249.94	98621.02	-	-	-	-
$11_{4,8} - 10_{4,7}$	$\upsilon_b = 1A$	240.4	234.40	98735.64	98736.0	0.38	31	
$11_{4,7} - 10_{4,6}$	$\upsilon_b = 1E$	233.2	-	98735.77	-	-	-	
$11_{4,8} - 10_{4,7}$	$\upsilon_b = 1E$	-	234.40	98738.68	98738.8	0.57	75	
$11_{4,7} - 10_{4,6}$	$\upsilon_b = 1A$	240.4	-	98739.06	-	-	-	
$12_{1,12} - 11_{1,11}$	$\upsilon_b = 1E$	297.2	229.03	107088.63	107088.5	0.52	50	C_2H_5OH ?
$12_{2,11} - 11_{2,10}$	$\upsilon_b = 1A$	-	229.03	107088.81	-	-	-	-
$12_{2,11} - 11_{2,10}$	$\upsilon_t = 1A$	294.5	235.76	107101.61	107101.2	0.34	37	
$12_{1,11} - 11_{1,10}$	$\upsilon_t = 1E$	-	235.76	107102.25	-	-	-	
$12_{8,4} - 11_{8,3}$	$\upsilon_b = 1E$	165.6	272.74	107251.81	107252.3	0.53	40	
$12_{8,5} - 11_{8,4}$	$\upsilon_b = 1E$	-	-	107252.50	-	-	-	
$12_{8,5} - 11_{8,3}$	$\upsilon_b = 1A$	-	-	107252.56	-	-	-	
$12_{8,4} - 11_{8,4}$	$\upsilon_b = 1A$	-	-	107252.93	-	-	-	
$12_{8,5} - 11_{8,4}$	$\upsilon_t = 1E$	148.1	284.97	107420.75	107420.9	0.80	40	(d)
$12_{8,4} - 11_{8,3}$	$\upsilon_t = 1E$	-	-	107421.34	-	-	-	-
$12_{8,5} - 11_{8,3}$	$\upsilon_t = 1A$	-	-	107421.59	-	-	-	-
$12_{8,4} - 11_{8,4}$	$\upsilon_t = 1A$	-	-	107421.66	-	-	-	-
$15_{4,12} - 14_{4,11}$	$\upsilon_t = 1A$	333.4	257.47	134571.52	134571.2	(c)	≤ 10	(c)
$15_{3,12} - 14_{3,11}$	$\upsilon_t = 1E$	329.8	257.47	134576.01	-	-	-	-
$15_{3,13} - 14_{3,12}$	$\upsilon_t = 1A$	349.5	251.67	134589.47	134590.2	0.46	60	$HCOOCH_3\upsilon_t = 1$
$15_{2,13} - 14_{2,12}$	$\upsilon_t = 1E$	-	-	134590.45	-	-	-	-
$15_{6,10} - 14_{6,9}$	$\upsilon_b = 1E$	318.4	255.87	134616.20	134616.1	3.23	135	(d)
$15_{6,9} - 14_{6,8}$	$\upsilon_b = 1E$	-	-	134616.38	-	-	-	-
$15_{5,11} - 14_{5,10}$	$\upsilon_b = 1A$	297.7	255.87	134616.44	-	-	-	-
$15_{5,10} - 14_{5,9}$	$\upsilon_b = 1A$	-	-	134616.58	-	-	-	-
$15_{11,5} - 14_{11,4}$	$\upsilon_b = 1E$	140.1	326.77	134640.95	134640.4	1.93	257	
$15_{11,5} - 14_{11,3}$	$\upsilon_b = 1A$	-	-	134641.10	-	-	-	
$15_{11,4} - 14_{11,3}$	$\upsilon_b = 1E$	-	-	134641.11	-	-	-	
$15_{11,4} - 14_{11,4}$	$\upsilon_b = 1A$	-	-	134641.12	-	-	-	
$15_{12,4} - 14_{12,3}$	$\upsilon_b = 1E$	104.7	343.90	134648.79	134648.1	2.37	132	(d)
$15_{12,3} - 14_{12,2}$	$\upsilon_b = 1E$	-	-	134648.90	-	-	-	-
$15_{12,4} - 14_{12,2}$	$\upsilon_b = 1A$	-	-	134648.98	-	-	-	-
$15_{12,3} - 14_{12,3}$	$\upsilon_b = 1A$	-	-	134649.00	-	-	-	-
$15_{10,6} - 14_{10,5}$	$\upsilon_b = 1E$	175.0	311.15	134650.29	-	-	-	-
$15_{10,6} - 14_{10,4}$	$\upsilon_b = 1A$	-	-	134650.34	-	-	-	-
$15_{10,5} - 14_{10,5}$	$\upsilon_b = 1A$	-	-	134650.34	-	-	-	-
$15_{10,5} - 14_{10,4}$	$\upsilon_b = 1E$	-	-	134650.49	-	-	-	-
$15_{13,3} - 14_{13,2}$	$\upsilon_b = 1E$	69.2	362.56	134666.30	131667.6	(c)	≤ 10	(c)
$15_{13,2} - 14_{13,1}$	$\upsilon_b = 1E$	-	-	134666.33	-	-	-	-
$15_{13,3} - 14_{13,1}$	$\upsilon_b = 1A$	-	-	134666.49	-	-	-	-
$15_{13,2} - 14_{13,2}$	$\upsilon_b = 1A$	-	-	134666.50	-	-	-	-
$15_{9,7} - 14_{9,5}$	$\upsilon_b = 1A$	209.4	297.07	134703.14	134702.7	0.98	103	

continued on next page

Table 3. Detected transitions of excited CH_3CH_2CN ($\upsilon_b = 1$ and $\upsilon_t = 1$) in W51 e2 – continued from previous page

Transition	State	$S\mu^2$ (D^2)	E_l (cm^{-1})	Frequency (MHz)	Obs. frequency[a] (MHz)	$\int T_{mb}\Delta v$[b] ($K.km.s^{-1}$)	T_{mb} (mK)	Comment
$15_{9,6} - 14_{9,6}$	$\upsilon_b = 1A$	-	-	134703.26	-	-	-	
$15_{9,7} - 14_{9,6}$	$\upsilon_b = 1E$	-	-	134703.45	-	-	-	
$15_{9,6} - 14_{9,5}$	$\upsilon_b = 1E$	-	-	134703.54	-	-	-	
$23_{0,23} - 22_{0,22}$	$\upsilon_b = 1E$	514.8	280.29	198463.40	198465.5	4.17	348	unidentified species
$23_{0,23} - 22_{0,22}$	$\upsilon_b = 1A$	-	-	198463.42	-	-	-	-
$23_{4,19} - 22_{4,18}$	$\upsilon_b = 1E$	485.2	293.79	207396.15	207397.5	8.58	758	$HCOOCH_3\upsilon_t = 1$
$23_{4,20} - 22_{4,19}$	$\upsilon_b = 1A$	-	293.79	207396.27	-	-	-	-
$23_{1,22} - 22_{1,21}$	$\upsilon_t = 1A$	502.5	290.47	207415.76	207240.2	6.69	568	$HCOOCH_3\upsilon_t = 1$
$23_{1,23} - 22_{1,22}$	$\upsilon_t = 1E$	-	290.47	207417.59	-	-	-	-
$24_{0,24} - 23_{1,23}$	$\upsilon_t = 1E$	188.2	293.36	207446.75	207446.0	(c)	≤ 15	C_2H_5OH
$24_{0,24} - 23_{1,23}$	$\upsilon_b = 1A$	186.9	293.36	207447.53	-	-	-	-
$24_{11,14} - 23_{11,13}$	$\upsilon_t = 1E$	325.5	393.52	215133.09	215132.5	(c)	≤ 380	unknown species
$24_{11,13} - 23_{11,12}$	$\upsilon_t = 1E$	-	-	215133.41	-	-	-	-
$24_{11,14} - 23_{11,12}$	$\upsilon_t = 1A$	-	-	215134.13	-	-	-	-
$24_{11,13} - 23_{11,13}$	$\upsilon_t = 1A$	-	-	215134.19	-	-	-	-
$25_{4,21} - 24_{4,20}$	$\upsilon_b = 1E$	511.8	307.94	225715.53	225714.7	(c)	≤ 228	(c)
$25_{4,22} - 24_{4,21}$	$\upsilon_b = 1A$	-	-	225715.61	-			
$27_{4,23} - 26_{4,22}$	$\upsilon_b = 1E$	534.4	323.30	244142.10	244139.3	3.94	288	
$27_{4,24} - 26_{4,23}$	$\upsilon_b = 1A$	-	-	244142.13	-	-	-	
$28_{1,27} - 27_{1,26}$	$\upsilon_t = 1A$	539.3	327.94	250318.38	250316.2	2.7	298	
$28_{2,27} - 27_{2,26}$	$\upsilon_t = 1E$	269.5	327.94	250319.81	-	-	-	
$28_{2,27} - 27_{2,26}$	$\upsilon_t = 1E$	-	-	250319.81	-	-	-	
$28_{15,13} - 27_{15,12}$	$\upsilon_b = 1E$	273.8	486.17	251372.86	251373.7	(c)	≤ 10	(c)
$28_{15,14} - 27_{15,13}$	$\upsilon_b = 1E$	-	-	251373.06	-	-	-	-
$28_{15,14} - 27_{15,12}$	$\upsilon_b = 1A$	-	-	251373.29	-	-	-	-
$28_{15,13} - 27_{15,13}$	$\upsilon_b = 1A$	-	-	251373.32	-	-	-	-

[a]Observed frequencies for a systemic velocity of $V_{lsr} = 57$ km/s.
[b]The line width is of the order of 7-8 $km.s^{-1}$.
[c]Line within the noise, a gaussian fit could not be made, constrains the abundance of excited ethyl cyanide.
[d]Very broad lines, ($\Delta v \geq 15 km.s^{-1}$), due to the blending of several excited ethyl cyanide transitions and/or to the blending with an unknown species.
The dashes indicates that the value is the same as the one in the previous line.